

# Quantum Monte Carlo Calculations of Light Nuclei Using Chiral Potentials

J. E. Lynn,<sup>1,\*</sup> J. Carlson,<sup>1</sup> E. Epelbaum,<sup>2</sup> S. Gandolfi,<sup>1</sup> A. Gezerlis,<sup>3</sup> and A. Schwenk<sup>4,5</sup>

<sup>1</sup>*Theoretical Division, Los Alamos National Laboratory, Los Alamos, New Mexico 87545, USA*

<sup>2</sup>*Institut für Theoretische Physik II, Ruhr-Universität Bochum, 44780 Bochum, Germany*

<sup>3</sup>*Department of Physics, University of Guelph, Guelph, Ontario, N1G 2W1, Canada*

<sup>4</sup>*Institut für Kernphysik, Technische Universität Darmstadt, 64289 Darmstadt, Germany*

<sup>5</sup>*ExtreMe Matter Institute EMMI, GSI Helmholtzzentrum für Schwerionenforschung GmbH, 64291 Darmstadt, Germany*

We present the first Green's function Monte Carlo calculations of light nuclei with nuclear interactions derived from chiral effective field theory up to next-to-next-to-leading order. Up to this order, the interactions can be constructed in a local form and are therefore amenable to quantum Monte Carlo calculations. We demonstrate a systematic improvement with each order for the binding energies of  $A = 3$  and  $A = 4$  systems. We also carry out the first few-body tests to study perturbative expansions of chiral potentials at different orders, finding that higher-order corrections are more perturbative for softer interactions. Our results confirm the necessity of a three-body force for correct reproduction of experimental binding energies and radii, and pave the way for studying few- and many-nucleon systems using quantum Monte Carlo methods with chiral interactions.

PACS numbers: 21.60.-n, 21.10.-k, 21.30.-x, 21.60.De

Important advances in our knowledge of light nuclei have been possible in recent years by using sophisticated numerical techniques like hyperspherical harmonics, the no-core shell model, and the Green's function Monte Carlo (GFMC) method. In particular, the nuclear GFMC method is one of the most accurate methods used to calculate the ground and excited state energies and other properties of light nuclei with mass number  $A \leq 12$  by using realistic nuclear Hamiltonians [1–7] based on the Argonne  $v_{18}$  two-body potential [8] and the Urbana/Illinois models of three-body forces [9, 10]. Despite the many successes of the nuclear GFMC method, until now it has been limited to modern phenomenological potentials. Interactions derived from chiral effective field theory (EFT) [11, 12] provide a direct connection between *ab initio* nuclear structure calculations and the underlying theory of strong interactions, quantum chromodynamics (QCD). These potentials have been successfully used in various regions of the nuclear landscape: from structure and reactions of light nuclei [13–15] to medium-mass nuclei [16–21] to infinite matter [22–26]. In this work, we combine, for the first time, the accurate nuclear GFMC machinery with chiral EFT interactions, which makes possible the first few-body studies of higher-order corrections in the chiral expansion.

The GFMC method is an exact method for studying nuclei with chiral interactions, because it works with the interactions in their bare form; that is, the Hamiltonian does not need to be softened by using renormalization group or other techniques [27]. Therefore, GFMC calculations of light nuclei with chiral EFT interactions will also be important to benchmark calculations using other methods that rely on such techniques. Until recently, nucleon-nucleon (NN) interactions derived from chiral EFT have been nonlocal, a feature which naturally results from the construction of these interactions

in momentum space where locality is not typically an important consideration. For many nuclear structure methods, nonlocal interactions do not pose any problems. In the case of the GFMC method, however, nonlocality poses nontrivial technical challenges. Sources of nonlocality in chiral EFT include the regulator choices, momentum-dependent contact interactions, and higher-order pion exchanges and relativistic contributions. The latter two appear only at next-to-next-to-next-to-leading order ( $N^3\text{LO}$ ) and beyond. Up to next-to-next-to-leading order ( $N^2\text{LO}$ ), the other two sources can be eliminated by choosing local regulators and an appropriate set of contact interactions as discussed in Ref. [24]. This opens up GFMC calculations of light nuclei with chiral potentials.

In this Letter, we discuss the first GFMC calculations of light nuclei for  $A \leq 4$  using NN interactions derived from chiral EFT. We present a systematic study of the ground-state energies at leading order (LO), next-to-leading order (NLO), and  $N^2\text{LO}$  and study the cutoff dependence at each order. We first briefly review the GFMC method and discuss the interaction used herein. Then we present our results for the  $A \leq 4$  systems and discuss the perturbative expansion of these forces at different values of the regulator cutoff.

The GFMC method consists of propagating in imaginary time  $t$  a trial wave function  $|\Psi_T\rangle$  to extract the ground-state wave function  $|\Psi_0\rangle$ . In the long imaginary-time limit, one has

$$\lim_{t \rightarrow \infty} e^{-Ht} |\Psi_T\rangle \rightarrow |\Psi_0\rangle, \quad (1)$$

with  $H$  the Hamiltonian of the system, if  $|\Psi_T\rangle$  is not orthogonal to  $|\Psi_0\rangle$ . Ground-state and low-lying excited-state observables are calculated by stochastic integration of the matrix elements  $\langle \Psi_T | O e^{-Ht} | \Psi_T \rangle$ , with  $O$  some observable. For reviews of the method, see, for example, Refs. [2, 4]. For the sampling of the propagator,  $e^{-Ht}$ ,

the standard GFMC method relies on locality of the potential. Though some progress has been made on this front [28, 29], it remains technically challenging to sample nonlocal terms by using the GFMC method without introducing large statistical errors. Local chiral EFT interactions allow for the use of the GFMC method with a minimum of further complications to calculate the propagator; however, a careful optimization of the two-body correlations which enter the wave function is necessary to account for the new potentials (as these are considerably different from the harder Argonne family of potentials). An attempt to develop a quantum Monte Carlo method to deal with nonlocal nuclear forces has been presented in Ref. [30] using the soft N<sup>2</sup>LO potential of Ref. [31]. Auxiliary-field quantum Monte Carlo calculations for a chiral interaction with a sharp cutoff were recently presented in Ref. [32].

We first clarify the notions of local and nonlocal interactions. If  $\mathbf{p} = (\mathbf{p}_1 - \mathbf{p}_2)/2$  and  $\mathbf{p}' = (\mathbf{p}'_1 - \mathbf{p}'_2)/2$  are the incoming and outgoing relative momenta of the nucleon pair, respectively, it is convenient to work in terms of the momentum transfer  $\mathbf{q} = \mathbf{p}' - \mathbf{p}$  and the momentum transfer in the exchange channel  $\mathbf{k} = (\mathbf{p}' + \mathbf{p})/2$ . When Fourier transformed, terms with  $\mathbf{q}$  lead to local interactions that depend only on the interparticle distance  $\mathbf{r}$ . However, terms with  $\mathbf{k}$  are nonlocal contributions depending on  $\nabla_{\mathbf{r}}$  that complicate the sampling of the propagator in the GFMC method. The only exception to this is the spin-orbit term, which contains a  $\mathbf{q} \times \mathbf{k}$  term that can be included in the GFMC propagator [2].

Chiral EFT provides a systematic expansion for nuclear forces and predicts a hierarchy of two- and many-nucleon interactions [11, 12]. At a given order, the interactions receive contributions from pion exchanges, which make up the long- and intermediate-range parts, as well as from short-range contact interactions. In particular, up to N<sup>2</sup>LO, the unregulated one- and two-pion-exchange contributions [33, 34] are local. To construct local chiral potentials, Refs. [24, 35] regulated the pion-exchange contributions with a regulator directly in coordinate space  $f_{\text{long}}(r) = 1 - e^{-(r/R_0)^4}$ , where  $R_0$  is a cutoff. We use  $R_0$  of 1.0, 1.1, and 1.2 fm, which approximately correspond to momentum cutoffs 500, 450, and 400 MeV, respectively. These values are obtained by Fourier transforming the regulator function, integrating over all momenta, and identifying the result with a sharp cutoff [35]. In addition, following Ref. [34], we employ for the two-pion-exchange contributions, a spectral-function regularization with cutoff  $\tilde{\Lambda}$  (we will use  $\tilde{\Lambda} = 1000$  MeV). The dependence on  $\tilde{\Lambda}$  is very weak [35], as we will demonstrate comparing to results for  $\tilde{\Lambda} = 1400$  MeV. For the short-range interactions, the local chiral potentials of Refs. [24, 35] select from the overcomplete set of operators ones that are local in coordinate space. This is possible up to N<sup>2</sup>LO; at N<sup>3</sup>LO, a number of nonlocal interactions will survive. For these higher-order interactions,

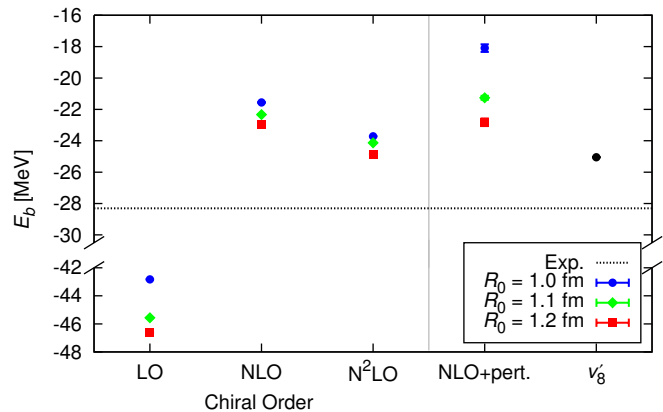


FIG. 1. (color online). <sup>4</sup>He binding energies ( $E_b$ ) at LO, NLO, and N<sup>2</sup>LO compared with experiment and with the Argonne  $v_8^s$  energy. Also shown is a first-order perturbation-theory calculation of the N<sup>2</sup>LO binding energy using the wave function at NLO:  $E_{\text{NLO}} + V_{\text{pert}}$ . See Eq. (2) and the discussion that follows. The GFMC statistical errors are generally smaller than the points.

we expect that they can be included perturbatively in the GFMC calculation, as is done with nonlocal parts in the Argonne  $v_{18}$  potential already [2]. The short-range interactions are then regulated with a regulator  $\sim e^{-(r/R_0)^4}$  complementary to the long-range one.

Interactions derived from chiral EFT are expected to show an order-by-order improvement or convergence. However, note that a calculation at N<sup>2</sup>LO with only two-body forces is incomplete, as three-body forces enter at this order. For each nucleus, we perform calculations at LO, NLO, and N<sup>2</sup>LO, varying the cutoff  $R_0$  from 1.0 to 1.2 fm. In Fig. 1 and Tables I to III, we present the GFMC results for the binding energies of the  $A = 3$  and  $A = 4$  nuclei for the various chiral potentials (the Coulomb potential is also included). As the chiral order increases, we can see a reduction in the theoretical uncertainty coming from the  $R_0$  variation. For example, for <sup>4</sup>He, the bands are  $\sim 3.8$  MeV,  $\sim 1.4$  MeV, and  $\sim 1.1$  MeV at LO, NLO, and N<sup>2</sup>LO, respectively. For <sup>4</sup>He at N<sup>2</sup>LO, we also used the spectral-function cutoff of  $\tilde{\Lambda} = 1400$  MeV with  $R_0 = 1.0$  fm and  $R_0 = 1.2$  fm. These calculations lowered the <sup>4</sup>He binding energy by 0.41 MeV ( $\sim 2\%$ ) and 0.46 MeV ( $\sim 2\%$ ), respectively (compared to the case with  $\tilde{\Lambda} = 1000$  MeV), which demonstrates a weak dependence on  $\tilde{\Lambda}$ . The calculated radii are consistent with the general trend in the binding energies: that is, at LO, the nuclei are significantly overbound, and the corresponding radii are too small compared to experiment; at NLO, the nuclei are underbound, and the radii are larger than experiment; at N<sup>2</sup>LO, the nuclei are still underbound, but closer to experiment, and the corresponding radii are smaller (closer to experiment).

The LO calculations bear additional discussion since, as Fig. 1 and Tables I to III show, we find that the nuclei

are significantly overbound: by as much as  $\sim 65\%$  of the experimental binding energy in the case of  ${}^4\text{He}$  with the cutoff at  $R_0 = 1.2$  fm. In the LO case, there are only two low-energy couplings, and the phase shifts are fit only up to  $E_{\text{lab}} = 50$  MeV; therefore, the effective-range physics is not reproduced and the potential is too attractive [35]. Since we expect the lightest nuclei with  $A = 2$  and  $A = 3$  to be least sensitive to higher energy scales, we might expect that these nuclei are less overbound than  ${}^4\text{He}$ . This trend is, indeed, borne out. At LO,  ${}^3\text{He}$  and  ${}^3\text{H}$  are overbound by as much as  $\sim 41\%$  and  $\sim 36\%$ , respectively (compared with the  $\sim 65\%$  for  ${}^4\text{He}$ ). The deuteron is underbound by  $\sim 9\%$  [35].

The chiral EFT expansion is an expansion in powers of momentum or of the pion mass  $\sim Q$  over a breakdown scale  $\Lambda_b$ . As we increase the chiral order, we expect suppression of the contributions from higher orders by powers of  $Q/\Lambda_b$ . It is clear from the results presented in Fig. 1 and Tables I to III that the NLO contribution is an important correction to the LO results. But the same results suggest that the contributions from N<sup>2</sup>LO are small relative to the NLO contributions. There is also evidence from calculations of the neutron-matter energy using chiral potentials that suggests perturbative behavior of chiral interactions [24, 25]. Therefore, it seems reasonable to attempt first-order perturbation theory for the  $A \leq 4$  nuclei, treating the difference in the potentials as a perturbation:

$$V_{\text{pert}} = V_{\text{N}^2\text{LO}} - V_{\text{NLO}}. \quad (2)$$

The results of these calculations for  ${}^4\text{He}$  are shown in Fig. 1. For each of the three values of the cutoff, we find the first-order contribution to be positive. The smallest correction comes in the  $R_0 = 1.2$  fm case as might be expected. (Larger  $R_0$  corresponds to lower  $\Lambda$  in momentum space, so that  $R_0 = 1.2$  fm is the softest potential used.) It would, of course, be desirable to com-

TABLE I. Binding energies and point proton radii for  ${}^4\text{He}$ . The errors given are statistical GFMC uncertainties. The experimental binding energy and root-mean-square (rms) point proton radius are  $E_b = -28.31$  MeV and  $\sqrt{\langle r_{\text{pt}}^2 \rangle} = 1.45$  fm, respectively.

Order	$R_0$ [fm]	$E_b$ [MeV]	$\sqrt{\langle r_{\text{pt}}^2 \rangle}$ [fm]
LO	1.0	-42.83(1)	1.02(1)
	1.1	-45.57(2)	1.00(1)
	1.2	-46.62(1)	1.00(1)
NLO	1.0	-21.56(1)	1.57(1)
	1.1	-22.33(1)	1.54(1)
	1.2	-22.94(6)	1.53(1)
N <sup>2</sup> LO	1.0	-23.72(1)	1.52(1)
	1.1	-24.13(1)	1.50(1)
	1.2	-24.86(1)	1.47(1)

TABLE II. Binding energies and point proton radii for  ${}^3\text{He}$ . The errors given are statistical GFMC uncertainties. The experimental binding energy and rms point proton radius are  $E_b = -7.72$  MeV and  $\sqrt{\langle r_{\text{pt}}^2 \rangle} = 1.76$  fm, respectively.

Order	$R_0$ [fm]	$E_b$ [MeV]	$\sqrt{\langle r_{\text{pt}}^2 \rangle}$ [fm]
LO	1.0	-10.42(1)	1.36(1)
	1.1	-10.78(1)	1.36(1)
	1.2	-10.88(1)	1.36(1)
NLO	1.0	-6.35(2)	1.92(2)
	1.1	-6.56(1)	1.90(2)
	1.2	-6.67(1)	1.88(1)
N <sup>2</sup> LO	1.0	-6.78(1)	1.87(2)
	1.1	-6.90(1)	1.84(1)
	1.2	-7.01(1)	1.82(1)

TABLE III. Binding energies and point proton radii for  ${}^3\text{H}$ . The errors given are statistical GFMC uncertainties. The experimental binding energy and rms point proton radius are  $E_b = -8.48$  MeV and  $\sqrt{\langle r_{\text{pt}}^2 \rangle} = 1.59$  fm, respectively.

Order	$R_0$ [fm]	$E_b$ [MeV]	$\sqrt{\langle r_{\text{pt}}^2 \rangle}$ [fm]
LO	1.0	-11.00(1)	1.27(1)
	1.1	-11.42(1)	1.26(1)
	1.2	-11.54(1)	1.27(1)
NLO	1.0	-7.10(1)	1.62(3)
	1.1	-7.25(2)	1.62(3)
	1.2	-7.35(1)	1.64(3)
N <sup>2</sup> LO	1.0	-7.55(1)	1.61(2)
	1.1	-7.63(1)	1.61(3)
	1.2	-7.74(1)	1.58(2)

pute higher-order perturbative corrections; however, it is difficult to obtain the second-order result or beyond.

We can, however, study first-, second-, and third-order perturbation-theory calculations for the deuteron. The methods developed in Refs. [28, 29] allow for the determination of the first  $N$  excited states of the deuteron. In the calculations discussed here,  $N \sim 800$ , giving truncation errors of less than  $10^{-10}$  MeV. Table IV shows the results of these calculations with the NLO and N<sup>2</sup>LO potentials with three different cutoffs. The first-order correction is positive and varies from 12% to 33% of the NLO deuteron binding energy for  $R_0 = 1.2$ –1.0 fm. The corrections at second and third order are both negative and range from 13% – 31% (at second order) and from 0.46% to 0.93% (at third order). The  $R_0 = 1.0$  fm case has the largest corrections at each order in the perturbation expansion; the  $R_0 = 1.2$  fm case has the smallest. There is some evidence, then, that the perturbative expansion for  $V_{\text{pert}}$  is converging in each case but faster for the softer potentials.

The perturbative check we have presented treats the difference in the fitted potentials at N<sup>2</sup>LO and NLO as a

TABLE IV. Perturbation calculations for  ${}^2\text{H}$  using the NLO and  $\text{N}^2\text{LO}$  potentials. The notation  $E_{\text{NLO}}$  indicates the ground-state energy of the NLO Hamiltonian.  $V_{\text{pert}}^{(n)}$  indicates the sum of the perturbative corrections up to the  $n$ th order.

Calculation	$E_b$ [MeV]		
	$R_0 = 1.0$ fm	$R_0 = 1.1$ fm	$R_0 = 1.2$ fm
$E_{\text{NLO}}$	-2.15	-2.16	-2.16
$E_{\text{NLO}} + V_{\text{pert}}^{(1)}$	-1.44	-1.80	-1.90
$E_{\text{NLO}} + V_{\text{pert}}^{(2)}$	-2.11	-2.17	-2.18
$E_{\text{NLO}} + V_{\text{pert}}^{(3)}$	-2.13	-2.18	-2.19
$E_{\text{N}^2\text{LO}}$	-2.21	-2.21	-2.20

perturbation, Eq. (2). We have also tested whether the new interactions entering at  $\text{N}^2\text{LO}$  are perturbative. To this end, we take the NLO parts of the  $\text{N}^2\text{LO}$  potential and treat the higher-order interactions as a perturbation. In this approach, the deuteron and  ${}^4\text{He}$  are unbound at first order in perturbation theory. These results appear to be due to the large  $c_i$ 's which enter at  $\text{N}^2\text{LO}$ . This pattern may be different in a chiral EFT with explicit Delta degrees of freedom, where the  $\text{N}^2\text{LO}$   $c_i$ 's are natural.

In addition to the binding energies and radii, we have calculated one- and two-body distributions and display them in Figs. 2 and 3. The proton distribution is given by

$$\rho_{1,p}(r) = \frac{1}{4\pi r^2} \langle \Psi_0 | \sum_i \frac{1 + \tau_z(i)}{2} \delta(r - |\mathbf{r}_i - \mathbf{R}_{\text{c.m.}}|) | \Psi_T \rangle, \quad (3)$$

where  $\mathbf{r}_i$  is the position of the  $i$ th nucleon,  $\mathbf{R}_{\text{c.m.}}$  is the center-of-mass of the nucleus, and  $\tau_z(i)/2$  is the  $z$  component of the isospin of the  $i$ th nucleon. We have calculated the two-body distribution functions in the  $T = 1$  isospin state, defined as

$$\rho_2^{(T=1)}(r) = \frac{3\rho_{2,1}(r) + \rho_{2,\tau\cdot\tau}(r)}{4}, \quad (4)$$

where

$$\rho_{2,o}(r) = \frac{1}{4\pi r^2} \langle \Psi_0 | \sum_{i < j} O_{ij} \delta(r - |\mathbf{r}_{ij}|) | \Psi_T \rangle. \quad (5)$$

In Figs. 2 and 3, it is clear that for distances  $r \gtrsim 1.5$  fm the NLO,  $\text{N}^2\text{LO}$ , and Argonne  $v_8^s$  distributions are very similar. At short distances ( $r \lesssim 1.5$  fm) the LO distributions are significantly larger than the distributions calculated with the other interactions. In Fig. 3, the different short-range behavior of the chiral forces and the Argonne  $v_8^s$  interaction is clear; the softer two-body  $T = 1$  NLO and  $\text{N}^2\text{LO}$  distributions (larger values of the distributions at the origin) suggest that short-range correlations between nucleons reflect the presence or absence of a hard core in the interaction [35]. In the lower

panel in Fig. 3, we show the dependence of  $\rho_2^{(T=1)}(r)$  on the cutoff by using the  $\text{N}^2\text{LO}$  potentials. The one-

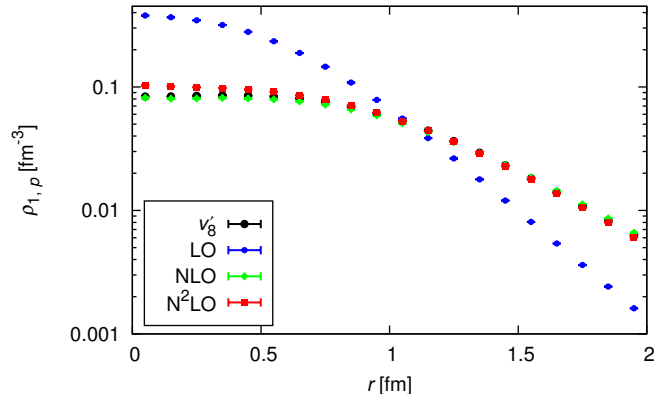


FIG. 2. (color online). One-body proton distributions for  ${}^4\text{He}$  with  $R_0 = 1.2$  fm at LO, NLO, and  $\text{N}^2\text{LO}$  compared with results for the Argonne  $v_8^s$  interaction. The error bars (generally smaller than the symbol size) are the statistical errors.

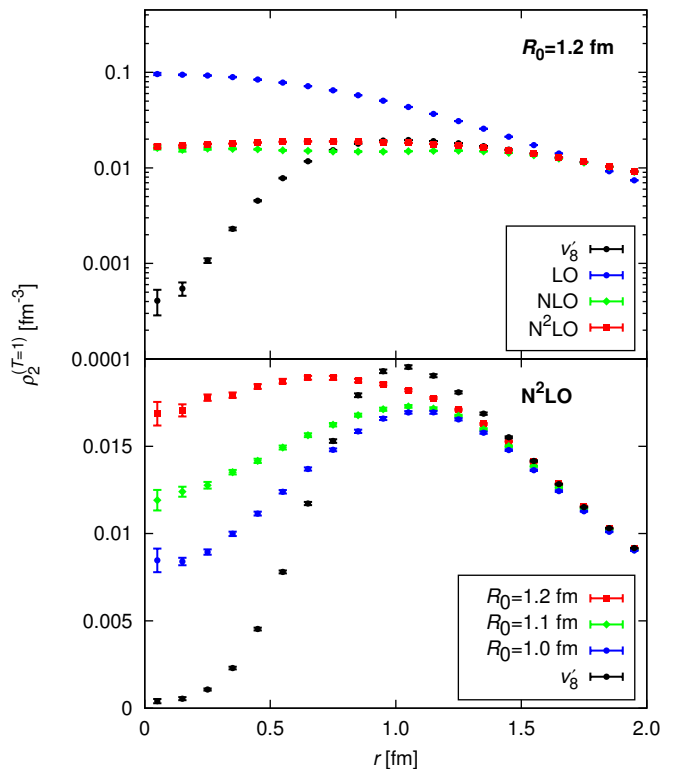


FIG. 3. (color online). Two-body  $T = 1$  distributions for  ${}^4\text{He}$  using chiral potentials and the Argonne  $v_8^s$  interaction. The top panel has the distributions calculated with  $R_0 = 1.2$  fm at LO, NLO, and  $\text{N}^2\text{LO}$ . The bottom panel shows the dependence of the  $\text{N}^2\text{LO}$  distribution at short distances on the cutoff  $R_0$ .

and two-body distributions lend further support to the discussion above about the overbinding of the nuclei at LO. Figures 2 and 3 imply that at LO the nucleons tend to be closer together than at higher order or with the phenomenological Argonne  $v'_8$  potential.

We have presented a systematic GFMC study of light nuclei  $A \leq 4$  with local NN interactions derived from chiral EFT up to N<sup>2</sup>LO. There is an order-by-order improvement for the binding energies, which is also shown by the weaker cutoff dependence. Our calculations confirm the necessity of a three-body force for nuclei with  $A \geq 3$ . We have also presented the first nonperturbative study of the interplay between different orders in the chiral expansion. We find that higher-order contributions are more perturbative for the softer potentials, and our calculations for the deuteron suggest that the perturbation expansion is converging to the result at N<sup>2</sup>LO. This study lays the groundwork for detailed nuclear GFMC studies of chiral EFT potentials for  $A \leq 12$  nuclei, which will also impact future simulations of larger systems with the auxiliary-field diffusion Monte Carlo method.

We thank S. Bacca, P. Navrátil, and I. Tews for useful discussions. The work of J.L., S.G., and J.C. is supported by the U.S. Department of Energy, Office of Nuclear Physics, and by the NUCLEI SciDAC program. The work of S.G. is also supported by the LANL LDRD program. The work of A.G. is supported by the Natural Sciences and Engineering Research Council of Canada. The work of A.S. is supported in part by ERC Grant No. 307986 STRONGINT, the Helmholtz Alliance Program of the Helmholtz Association Contract No. HA216/EMMI “Extremes of Density and Temperature: Cosmic Matter in the Laboratory,” and by computing resources at the Jülich Supercomputing Center. The work of E.E. is supported in part by ERC Grant No. 259218 NUCLEAREFT. Computational resources have been provided by Los Alamos Open Supercomputing. This research used also resources of the National Energy Research Scientific Computing Center (NERSC), which is supported by the Office of Science of the U.S. Department of Energy under Contract No. DE-AC02-05CH11231.

---

\* E-mail: joel.lynn@gmail.com

- [1] J. Carlson, Phys. Rev. C **36**, 2026 (1987).
- [2] B. S. Pudliner, V. R. Pandharipande, J. Carlson, S. C. Pieper, and R. B. Wiringa, Phys. Rev. C **56**, 1720 (1997).
- [3] R. B. Wiringa, S. C. Pieper, J. Carlson, and V. R. Pandharipande, Phys. Rev. C **62**, 014001 (2000).
- [4] S. C. Pieper and R. B. Wiringa, Annu. Rev. Nucl. Part. Sci. **51**, 53 (2001).
- [5] S. C. Pieper, K. Varga, and R. B. Wiringa, Phys. Rev. C **66**, 044310 (2002).
- [6] A. Lovato, S. Gandolfi, R. Butler, J. Carlson, E. Lusk, S. C. Pieper, and R. Schiavilla, Phys. Rev. Lett. **111**, 092501 (2013).
- [7] A. Lovato, S. Gandolfi, J. Carlson, S. C. Pieper, and R. Schiavilla, Phys. Rev. Lett. **112**, 182502 (2014).
- [8] R. B. Wiringa, V. G. J. Stoks, and R. Schiavilla, Phys. Rev. C **51**, 38 (1995).
- [9] B. S. Pudliner, V. R. Pandharipande, J. Carlson, and R. B. Wiringa, Phys. Rev. Lett. **74**, 4396 (1995).
- [10] S. C. Pieper, V. R. Pandharipande, R. B. Wiringa, and J. Carlson, Phys. Rev. C **64**, 014001 (2001).
- [11] E. Epelbaum, H.-W. Hammer, and U.-G. Meißner, Rev. Mod. Phys. **81**, 1773 (2009).
- [12] R. Machleidt and D. R. Entem, Phys. Rep. **503**, 1 (2011).
- [13] E. Epelbaum, H. Krebs, D. Lee, and U.-G. Meißner, Phys. Rev. Lett. **104**, 142501 (2010).
- [14] B. R. Barrett, P. Navrátil, and J. P. Vary, Prog. Part. Nucl. Phys. **69**, 131 (2013).
- [15] S. Bacca, N. Barnea, W. Leidemann, and G. Orlandini, Phys. Rev. Lett. **110**, 042503 (2013).
- [16] T. Otsuka, T. Suzuki, J. D. Holt, A. Schwenk, and Y. Akaishi, Phys. Rev. Lett. **105**, 032501 (2010).
- [17] H. Hergert, S. K. Bogner, S. Binder, A. Calci, J. Langhammer, R. Roth, and A. Schwenk, Phys. Rev. C **87**, 034307 (2013).
- [18] S. Binder, J. Langhammer, A. Calci, and R. Roth, Phys. Lett. B **736**, 119 (2013).
- [19] G. Hagen, T. Papenbrock, M. Hjorth-Jensen, and D. J. Dean, Rep. Prog. Phys. **77**, 096302 (2014).
- [20] V. Somà, A. Cipollone, C. Barbieri, P. Navrátil, and T. Duguet, Phys. Rev. C **89**, 031301 (2014).
- [21] F. Wienholtz *et al.*, Nature **498**, 346 (2013).
- [22] K. Hebeler and A. Schwenk, Phys. Rev. C **82**, 014314 (2010).
- [23] K. Hebeler, S. K. Bogner, R. J. Furnstahl, A. Nogga, and A. Schwenk, Phys. Rev. C **83**, 031301 (2011).
- [24] A. Gezerlis, I. Tews, E. Epelbaum, S. Gandolfi, K. Hebeler, A. Nogga, and A. Schwenk, Phys. Rev. Lett. **111**, 032501 (2013).
- [25] T. Krüger, I. Tews, K. Hebeler, and A. Schwenk, Phys. Rev. C **88**, 025802 (2013).
- [26] G. Hagen, T. Papenbrock, A. Ekström, K. A. Wendt, G. Baardsen, S. Gandolfi, M. Hjorth-Jensen, and C. J. Horowitz, Phys. Rev. C **89**, 014319 (2014).
- [27] S. K. Bogner, R. J. Furnstahl, and A. Schwenk, Prog. Part. Nucl. Phys. **65**, 94 (2010).
- [28] J. E. Lynn and K. E. Schmidt, Phys. Rev. C **86**, 014324 (2012).
- [29] J. E. Lynn, Ph.D. thesis, Arizona State University (2013).
- [30] A. Roggero, A. Mukherjee, and F. Pederiva, Phys. Rev. Lett. **112**, 221103 (2014).
- [31] A. Ekström, G. Baardsen, C. Forssén, G. Hagen, M. Hjorth-Jensen, G. R. Jansen, R. Machleidt, W. Nazarewicz, T. Papenbrock, J. Sarich, and S. M. Wild, Phys. Rev. Lett. **110**, 192502 (2013).
- [32] G. Wlazłowski, J. W. Holt, S. Moroz, A. Bulgac, and K. J. Roche, (2014), arXiv:1403.3753 [nucl-th].
- [33] N. Kaiser, R. Brockmann, and W. Weise, Nucl. Phys. A **625**, 758 (1997).
- [34] E. Epelbaum, W. Glöckle, and U.-G. Meißner, Eur. Phys. J. A **19**, 125 (2004).
- [35] A. Gezerlis, I. Tews, E. Epelbaum, M. Freunek, S. Gandolfi, K. Hebeler, A. Nogga, and A. Schwenk, (2014), arXiv:1406.0454 [nucl-th].